View metadata, citation and similar papers at core.ac.uk
brought to you by CORE
provided by PolyU Institutional Repository

Vortex sound in the presence of a low Mach number flow across a drum-like silencer

S. K. Tang[a)]
Department of Building Services Engineering, The Hong Kong Polytechnic University, Hong Kong, China

(Received 28 April 2010; revised 13 February 2011; accepted 16 February 2011)

The sound generated by a vortex propagating across a two-dimensional duct section with flexible walls (membranes) in an infinitely long rigid duct conveying a flow is investigated numerically using the matched asymptotic expansion technique and the potential theory. The effects of the initial vortex position, the mechanical properties of the flexible walls, and the mean flow on the sound generation are examined in detail. Results show that the presence of a vortex inside a uniform mean flow can strengthen or attenuate the sound generation, depending on the phase of the membrane vibration when the vortex starts vigorous interaction with the membranes and the strength of the mean flow. The results tend to imply that there is a higher chance of sound amplification when a vortex stream is moving closer to the lighter membrane under a relatively strong mean flow or when the mean flow is weak. The chances of sound amplification or attenuation are equal otherwise.
© *2011 Acoustical Society of America*. [DOI: 10.1121/1.3562567]

PACS number(s): 43.28.Ra, 43.40.Rj, 43.50.Nm [JWP] Pages: 2830–2840

I. INTRODUCTION

The air conditioning and ventilation system is one of the major noise sources in a modern heavily serviced commercial building. The noise from the air handling unit of the system, which basically consists of a powerful fan, propagates into the building interior through the ductwork which at the same time conveys the treated air to the occupied zones within the building. There are also exhaust fans which extract the used air inside the building out of the building. Duct noise control is therefore an important duty of a building services engineer.

The conventional method to attenuate these noises is by using dissipative silencers in which the porous materials inside them damp the noise by converting the acoustical energy into heat.[1] The acoustical performance of these materials at low frequencies is not satisfactory, and thus attenuating the low frequency noise from the fans in the air conditioning and ventilation ductwork by using porous materials is not cost-effective. The topic of low frequency duct noise attenuation has attracted the attentions of many researchers and engineers over the past few decades. There have been efforts on understanding the performances of various reactive components in the noise control[2,3] and on the use of combined dissipative and reactive methods for the noise attenuation.[4] Active cancellation methods using adaptive digital filters have also been explored (for instance, Canevet[5] and Nelson and Elliott[6]).

The use of vibro-acoustic technique for noise attenuation has also been investigated. Ford and McCormick[7] demonstrated theoretically the noise attenuation by a panel absorber. There were also studies focused on the interaction between flexible boundaries and sound (for instance, Frendi *et al.*[8] and Filippi *et al.*[9]). More recently, Huang[10] studied the effect of membrane vibration on the sound propagation in duct and proposed a drum-like silencer for low frequency duct noise attenuation.[11] However, flexible duct walls are also susceptible to excitation by flow turbulence and the flow as well. There are solid evidences showing that sound can be produced through the complicated interactions between flow turbulent eddies and pressure-releasing devices, such as flexible walls,[12,13] perforated screens,[14] and porous materials.[15] Such sound generations are expected to lower the performance of any duct noise control devices developed based on vibro-acoustic consideration.

Since turbulent flows are basically not amenable to analytical solutions, vortices are often used as a simplification for getting insights into the sound generation and the flow induced vibration of complicated flow-structure interactions. Typical examples of this branch of study include Crighton,[16] Howe,[17] and Obermeier.[18] The sound generated by a vortex interacting with two flexible duct boundaries backed by airtight cavities in the presence of a mean flow inside the duct is studied in detail in the present investigation. This configuration is analogous to that of the drum-like silencer of Huang and Choy.[11] The effects of asymmetric wall boundary properties on the sound generation are also examined. It is hoped that the present results can lead to increased understanding of the possible sound producing mechanisms when a vortex engages with a flexible structure in the presence of a low Mach number duct flow.

II. THEORETICAL DEVELOPEMENT

The flows inside the air conditioning and ventilation ductwork are practically of high Reynolds number but low Mach number, so that the effects of viscosity can be ignored for simplicity. Figure 1 shows the schematics and the nomenclatures adopted in the present study. An inviscid vortex with circulation Γ initially located far upstream of the flexible duct wall section propagates toward this duct

[a)]Author to whom correspondence should be addressed. Electronic mail: besktang@polyu.edu.hk

 0001-4966/2011/129(5)/2830/11/$30.00 © 2011 Acoustical Society of America

Redistribution subject to ASA license or copyright; see http://acousticalsociety.org/content/terms. Download to IP: 158.132.161.50 On: Fri, 27 Dec 2013 13:08:13

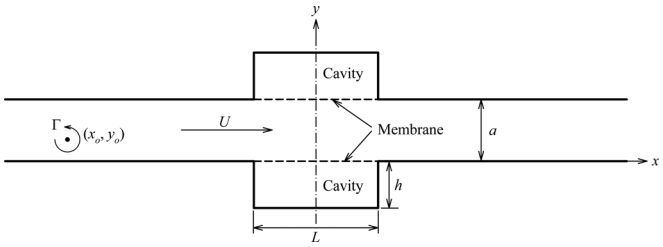

FIG. 1. Schematics of the present duct system and the nomenclature adopted.

section under the combined effects of the self-induced velocity and the mean flow U. The flexible walls are modeled as membranes with tension per unit length T, mass density m, and a damping coefficient D as in Huang[10] and in the previous investigations of the authors.[13,19] In the foregoing sections, a and (x_o, y_o) represent the width of the duct and the instantaneous vortex position, respectively. The length and height of the cavity are denoted by L and h, respectively.

A. Vortex velocity and membrane vibrations

For small membrane vibration magnitudes, the vibrating membranes are modeled as rigid boundaries with distributed fluctuating normal velocities as in Tang *et al.*[13] The complex flow potential at any position (x, y) inside a channel, W, due to a flow of velocity v into the channel through a tiny opening of width Δx at $x=0$, $y=0$ is[20]

$$W = \frac{v\Delta x}{\pi}\log\left[\sinh\left(\frac{\pi}{2a}(x+jy)\right)\right], \tag{1}$$

where $j=\sqrt{-1}$. It is straight-forward to show that the real part of W is

$$\mathrm{Re}(W) = \frac{v\Delta x}{2\pi}\{\log[\cosh(\pi x/a)-\cos(\pi y/a)]-\log(2)\}. \tag{2}$$

The fluid velocity at any point (x, y) along the duct in the present study induced by the membrane vibrations can therefore be estimated by an integration along the membranes

$$\begin{aligned} v(x,y) = {} & \frac{\hat{x}}{2a}\int_{-L/2}^{L/2}\left[\frac{v_l(x')\sinh(\pi(x'-x)/a)}{\cosh(\pi(x'-x)/a)-\cos(\pi(y-\eta_1)/a)}\right. \\ & \left.-\frac{v_u(x')\sinh(\pi(x'-x)a)}{\cosh(\pi(x'-x)/a+\cos(\pi(y-\eta_u)/a)}\right]dx' \\ & +\frac{\hat{y}}{2a}\int_{-L/2}^{L/2}\left[\frac{v_l(x')\sin(\pi(y-\eta_l)/a)}{\cosh(\pi(x'-x)/a)-\cos(\pi(y-\eta_l)/a)}\right. \\ & \left.+\frac{v_u(x')\sin(\pi(y-\eta_u)a)}{\cosh(\pi(x'-x)/a)+\cos(\pi(y-\eta_u)/a)}\right]dx', \end{aligned} \tag{3}$$

where η denotes the membrane displacement, $\hat{x}$ and $\hat{y}$ are the unit vectors in the x- and y-directions, respectively, x' is the distance within the membrane section, and v_l and v_u are the duct-side fluid velocities on the lower and upper membrane, respectively:[11]

$$v_l = \frac{\partial\eta_l}{\partial\tau}+U\frac{\partial\eta_l}{\partial x'} \quad \text{and} \quad v_u = \frac{\partial\eta_u}{\partial\tau}+U\frac{\partial\eta_u}{\partial x'}, \tag{4}$$

where τ denotes the time and the suffices u and l hereinafter denote the quantities related to the upper and lower membrane, respectively. The vortex velocity is

$$v_o = \left[U+\frac{\Gamma}{4a}\cot(\pi y/a)\right]\hat{x}+v(x_o,y_o). \tag{5}$$

The near field incompressible flow potential at any point (x, y) inside the duct is given by the general expression

$$\begin{aligned} \phi(x,y,\tau) = {} & \frac{\Gamma}{2\pi}\tan^{-1}\left[\tan\left(\frac{(a-y_o+y)\pi}{2a}\right)\tanh\left(\frac{(x-x_o)\pi}{2a}\right)\right] \\ & +\frac{\Gamma}{2\pi}\tan^{-1}\left[\tan\left(\frac{(a-y_o-y)\pi}{2a}\right)\tanh\left(\frac{(x-x_o)\pi}{2a}\right)\right] \\ & +\frac{1}{2\pi}\int_{-L/2}^{L/2}\left(\frac{\partial\eta_l}{\partial\tau}+U\frac{\partial\eta_l}{\partial x'}\right)\log[\cosh(\pi(x-x')/a) \\ & -\cos(\pi(y-\eta_l)/a)]dx'-\frac{1}{2\pi}\int_{-L/2}^{L/2}\left(\frac{\partial\eta_u}{\partial\tau}+U\frac{\partial\eta_u}{\partial x'}\right) \\ & \times\log[\cosh(\pi(x-x')/a)+\cos(\pi(y-\eta_u)/a)]dx' \\ & +Ux+\gamma(\tau), \end{aligned} \tag{6}$$

where γ is a sole function of time to be found through the matched asymptotic expansion discussed in Sec. II B. Similar technique of introducing a time variant to the flow potential has been employed by Cannell and Ffowcs Williams.[21] The first two terms on the right-hand-side of Eq. (6) are the potentials due to the vortex, which is obtained by the method of infinite images. The next two terms come from the membrane vibrations.

The vortex motion and the mean flow give rise to fluctuating pressure forces on the two membranes. The equations of motion governing the vibrations of the membranes are[13]

$$m\frac{\partial^2\eta_u}{\partial\tau^2} = T\frac{\partial^2\eta_u}{\partial x^2}-D\frac{\partial\eta_u}{\partial\tau}-(p_u^+-p_u^-) \tag{7a}$$

and

$$m\frac{\partial^2\eta_l}{\partial\tau^2} = T\frac{\partial^2\eta_l}{\partial x^2}-D\frac{\partial\eta_l}{\partial\tau}-(p_u^+-p_u^-), \tag{7b}$$

where p is the fluid pressure and the superscripts "+" and "−" represent the meaning of "above" and "below" the membrane, respectively. The linearized Bernoulli relationship gives[22]

$$p_l^* = -\rho\left(\frac{\partial\phi}{\partial\tau}+U\frac{\partial\phi}{\partial x}\right)_{y=\eta_l} \quad \text{and} \quad p_u^- = -\rho\left(\frac{\partial\phi}{\partial\tau}+U\frac{\partial\phi}{\partial x}\right)_{y=\eta_u}, \tag{8}$$

where ρ denotes ϕ near the field fluid density and the flow potential.

Following the work of Tang *et al.*[19] for vibration having frequency much lower than the first eigenmode frequency of the cavity such that the fluid pressure inside individual cavity can be assumed to be uniform

Redistribution subject to ASA license or copyright; see http://acousticalsociety.org/content/terms. Download to IP: 158.132.161.50 On: Fri, 27 Dec 2013 13:08:13

$$p_l^- = c^2\Delta\rho = -\frac{c^2\rho}{hL}\int_{-L/2}^{L/2}\eta_l dx \quad \text{and}$$

$$p_u^+ = -\frac{c^2\rho}{hL}\int_{-L/2}^{L/2}\eta_u dx, \tag{9}$$

where c is the speed of sound. The membranes are initially at rest such that $\eta_l = \eta_u = 0$. The vibration velocities and accelerations of membranes and the vortex velocity can then be estimated by integrating the coupled equations [Eqs. (3)–(9)] using standard numerical integration technique. The fourth order Runge-Kutta procedure is chosen for the present study.

It has been shown by Choy and Huang[23] that the change in tension because of the further extension of the membranes is practically not important and thus T is assumed to be constant. The membranes should have been stretched to a great extent in the beginning in order to maintain tension. In fact, the extensions of the membranes are less than 0.2% throughout the present investigation, such that the change in T can basically be ignored.

It should be noted that the possible vorticity production at the stationary edges of the membranes is not considered in the present study, given the very small membrane vibration magnitudes such that the flow singularity at the edges is not significant. This has been confirmed by the results of Choy and Huang[23] who showed good agreement between measurements and the theoretical deductions formulated without the vorticity production taken into account. However, such flow singularity is significant in the case of a vibrating piston[24] or a porous surface.[25]

B. Far field sound in flow duct

Inside a flow duct, the matching procedure is different from that for the free field radiation in the previous study of the author.[19] The wave equation in the presence of a low Mach number steady mean flow for plane wave far away from the near field is[17]

$$\frac{\partial}{\partial t}\left(\frac{\partial\phi}{\partial t}+U\frac{\partial\phi}{\partial x}\right)+U\frac{\partial}{\partial x}\left(\frac{\partial\phi}{\partial t}+U\frac{\partial\phi}{\partial x}\right)-c^2\frac{\partial^2\phi}{\partial x^2}=0$$
$$\Rightarrow \left(\frac{\omega}{c}\right)^2\Phi-\frac{2Mj\omega}{c}\frac{\partial\Phi}{\partial x}+(1-M^2)\frac{\partial^2\Phi}{\partial x^2}=0, \tag{10}$$

where t is the time, M is the Mach number ($=U/c$), and Φ is the time-Fourier transform of ϕ in the far field

$$\Phi=\int_{-\infty}^{\infty}\phi e^{-j\omega t}dt$$

The general solution of Eq. (10) is

$$\Phi = A\exp\left(-\frac{j\omega x}{c(1+M)}\right)+B\exp\left(\frac{j\omega x}{c(1-M)}\right) \tag{11}$$

which consists of a downstream and an upstream going wave having the complex magnitude A and B, respectively. This solution should match with the incompressible near field solution as $|x|\to\infty$, ϕ_∞, for very low frequency radiation where $\omega x/c\to 0$. For $x\to+\infty$, $B=0$ as there is no wave moving back toward the near field and from Eq. (6)

$$\varphi_{+\infty}=\frac{\Gamma}{2}\left(1-\frac{y_a}{a}\right)+\frac{1}{2a}\int_{-L/2}^{L/2}\left(\frac{\partial\eta_l}{\partial\tau}+U\frac{\partial\eta_l}{\partial x'}\right)(x-x')dx'$$
$$-\frac{1}{2a}\int_{-L/2}^{L/2}\left(\frac{\partial\eta_u}{\partial\tau}+U\frac{\partial\eta_u}{\partial x'}\right)(x-x')dx'+Ux+\gamma$$
$$\approx\frac{\Gamma}{2}\left(1-\frac{y_o}{a}\right)+\frac{x}{2a}\int_{-L/2}^{L/2}\left(\frac{\partial\eta_l}{\partial\tau}-\frac{\partial\eta_u}{\partial\tau}\right)dx'+Ux+\gamma \tag{12}$$

as $x\gg x'$. The matching of the time fluctuating part of $\phi_{+\infty}$ to the far field solution given in Eq. (11) with $\omega x/c\to 0$ and $M\to 0$ suggests to the leading order that

$$\gamma=\frac{c}{2a}\int_{-L/2}^{L/2}(\eta_u-\eta_l)dx', \tag{13}$$

and thus the complex value A is the time-Fourier transform of $\phi_{f,+\infty}$ where

$$\phi_{f,+\infty}=\frac{\Gamma}{2}\left(1-\frac{y_o}{a}\right)+\frac{c}{2a}\int_{-L/2}^{L/2}(\eta_u-\eta_l)dx'. \tag{14}$$

The downstream far field pressure, $p_{+\infty}$, is

$$p_{+\infty}=-\rho\left(\frac{\partial\phi_{f,+\infty}}{\partial t}+U\frac{\partial\phi_{f,+\infty}}{\partial x}\right)=-\frac{\rho}{1+M}\frac{\partial\phi_{f,+\infty}}{\partial t}$$
$$=-\frac{\rho}{1+M}\left[-\frac{\Gamma}{2a}\frac{\partial y_o}{\partial\tau}+\frac{c}{2a}\int_{-L/2}^{L/2}\frac{\partial}{\partial\tau}(\eta_u-\eta_l)dx'\right], \tag{15}$$

where $\phi_{f,+\infty}$ and the expression in the square bracket are evaluated at the retarded time $t-x/[c(1+M)]$. The first term in the square bracket represents the sound generated directly from the vortex transverse velocity, which is commonly found in duct vortex sound cases (for instance, Tang and Lau[15]), while the second one the plane wave generated by the volumetric fluid flow resulted from membrane vibrations. The latter is also commonly observed in low frequency duct noise study (for instance, Nelson and Elliott[6]). The factor $(1+M)$ is the modification of sound magnitude by the mean flow for downstream low frequency sound radiation in the ducted condition.[26] Similarly, one can obtain for $x\to-\infty$:

$$\phi_{f,-\infty}=-\frac{\Gamma}{2}\left(1-\frac{y_o}{a}\right)+\frac{c}{2a}\int_{-L/2}^{L/2}(\eta_u-\eta_l)dx' \tag{16}$$

and

$$p_{-\infty}=-\rho\left(\frac{\partial\phi_{f,-\infty}}{\partial t}+U\frac{\partial\phi_{f,-\infty}}{\partial x}\right)$$
$$=-\frac{\rho}{1-M}\frac{\partial\phi_{f,-\infty}}{\partial t}, \tag{17}$$

Redistribution subject to ASA license or copyright; see http://acousticalsociety.org/content/terms. Download to IP: 158.132.161.50 On: Fri, 27 Dec 2013 13:08:13

where the time derivative of $\phi_{f,-\infty}$ is evaluated at the retarded time $t+x/[c(1-M)]$. The vortex transverse motion creates a dipole radiation, while the volumetric flow induced by the membrane vibrations a monopole.

III. RESULTS AND DISCUSSIONS

As in the previous study of the author,[19] the mean flow is introduced abruptly into the duct. The membranes start to vibrate at the very beginning because of such mean flow excitation. The two membranes vibrate out-of-phase to effect the monopole radiation initially. These membrane vibrations are somewhat self-sustained due to resonance if the two membranes are identical.

All length scales in the present study are normalized by the duct width a and the velocities, including the speed of sound c, by Γ/a, which is set to be $0.1c$ and the mean flow velocity U is capped at $0.2c$ to ensure the low Mach number condition. The tension per unit length T, the damping coefficient D, and the membrane mass density m are normalized accordingly by $\rho a\Gamma$, $\rho\Gamma/a$, and ρa, respectively. It has been demonstrated by Huang and Choy[11] that D is very weak in practice, and thus its effects are not included in the present study. D is set to unity according to the information from Frendi *et al.*[8] for weak damping situation. The *in-vacuo* wave speed along the membrane $c_m=\sqrt{T/m}$ which is about $0.1c$ for practical membrane materials.[10] The extensions of the membranes are kept below 0.2% throughout the present study such that the change in T can be ignored.[23] In the present study, the length of the membrane L is set at 2 and the cavity height h at 0.5. The initial position of the vortex is located at $x_{oi}=-10$, unless otherwise specified.

A. Membrane vibrations and vortex dynamics

Figure 2 summarizes the effect of initial vortex height y_{oi} and U on the vortex path for $T=100$ and $m=100$. It can be observed from Fig. 2(a) that the vortex path for $y_{oi}=0.1$ in the absence of the mean flow is quite close to that of the corresponding case of Tang *et al.*[19] without the upper membrane when y_o is normalized by y_{oi}. It is believed that for smaller y_{oi}, the effects from the upper membrane are not significant and the corresponding results will be close to those shown in Tang *et al.*[19] It seems that the vortex path will eventually bend upward as U increases. However, it is strongly associated with the vibration phases of the membranes and is not straight-forward. It will be discussed in detail later.

The increase in the initial vortex height strengthens the effects of the upper membrane on the vortex motion as shown in Fig. 2(b). Without the mean flow, the vortex resumes back its original height after engaging with the membranes. However, unlike the case of Tang *et al.*,[19] there does not exist a well defined trend of the vortex path variation with U. The situation becomes even more acute when y_{oi} is increased to 0.4 [Fig. 2(c)]. Nevertheless, the vortex height variations are very small. It is ~6% for $y_{oi}=0.1$ but drops to less than 0.03% for $y_{oi}=0.4$. The pressure-releasing effect of the upper membrane tends to equalize that of the lower one on the vortex, resulting in weaker vortex transverse velocity than the cases studied previously by Tang *et al.*[19] The sound generated directly by the vortex motion is thus weakened as y_{oi} increases. This will be discussed in Sec. III B.

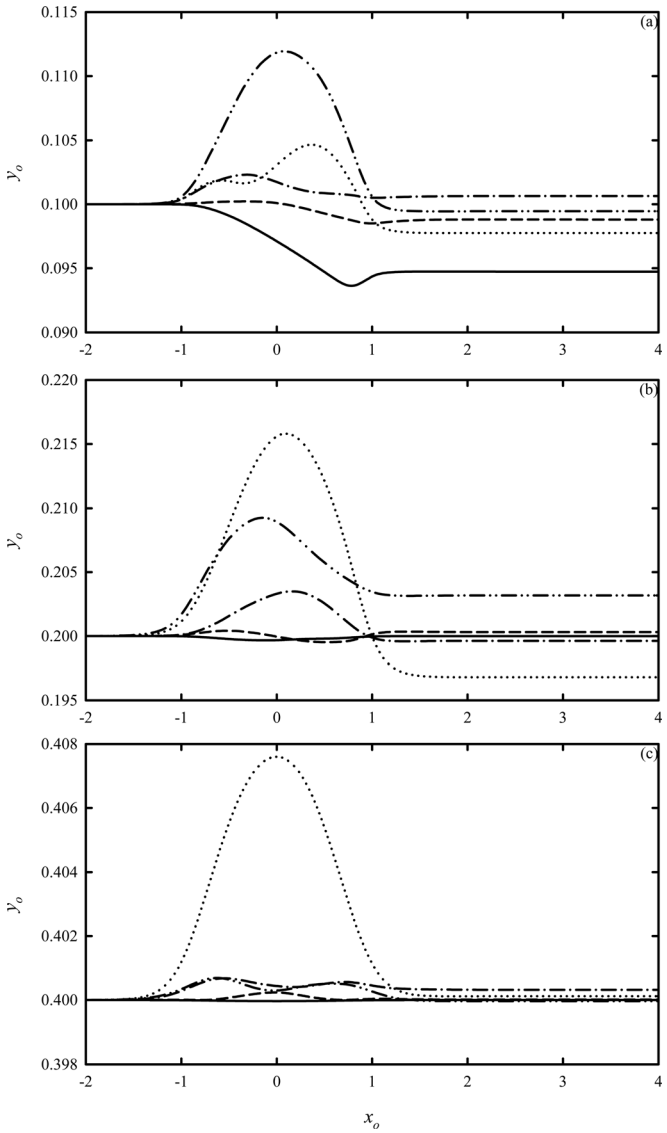

FIG. 2. Effects of the mean flow velocity and initial vortex height on the vortex path. (a) $y_{oi}=0.1$; (b) $y_{oi}=0.2$; (c) $y_{oi}=0.4$. ————: $U=0$; — — —: $U=0.5$; —·—: $U=1$; —··—: $U=1.5$; ·····: $U=2$. T = 100, $m=100$.

The observed smaller variation of the vortex path with increasing U is due to the phases of the membrane vibrations when the vortex starts engaging the membranes. Figures 3(a)–3(c) illustrate the vibrating velocities of the lower membrane for $y_{oi}=0.1$, $T=100$, $m=100$ and with $U=1.5$, 2, and 0.8, respectively. τ_0 denotes the time when the vortex flies over the plane $x=-1$, which is the leading edge of the membrane section. The dash lines represent the vortex longitudinal position x_o. At this y_{oi}, the effect from the upper membrane is weak when compared to that of the lower one. The membranes vibrate out-of-phase with each other before the vortex comes into the proximity of the membrane section (not shown here).

For the case with $U=1.5$, the lower membrane is moving upward basically over the period the vortex is flying over

Redistribution subject to ASA license or copyright; see http://acousticalsociety.org/content/terms. Download to IP: 158.132.161.50 On: Fri, 27 Dec 2013 13:08:13

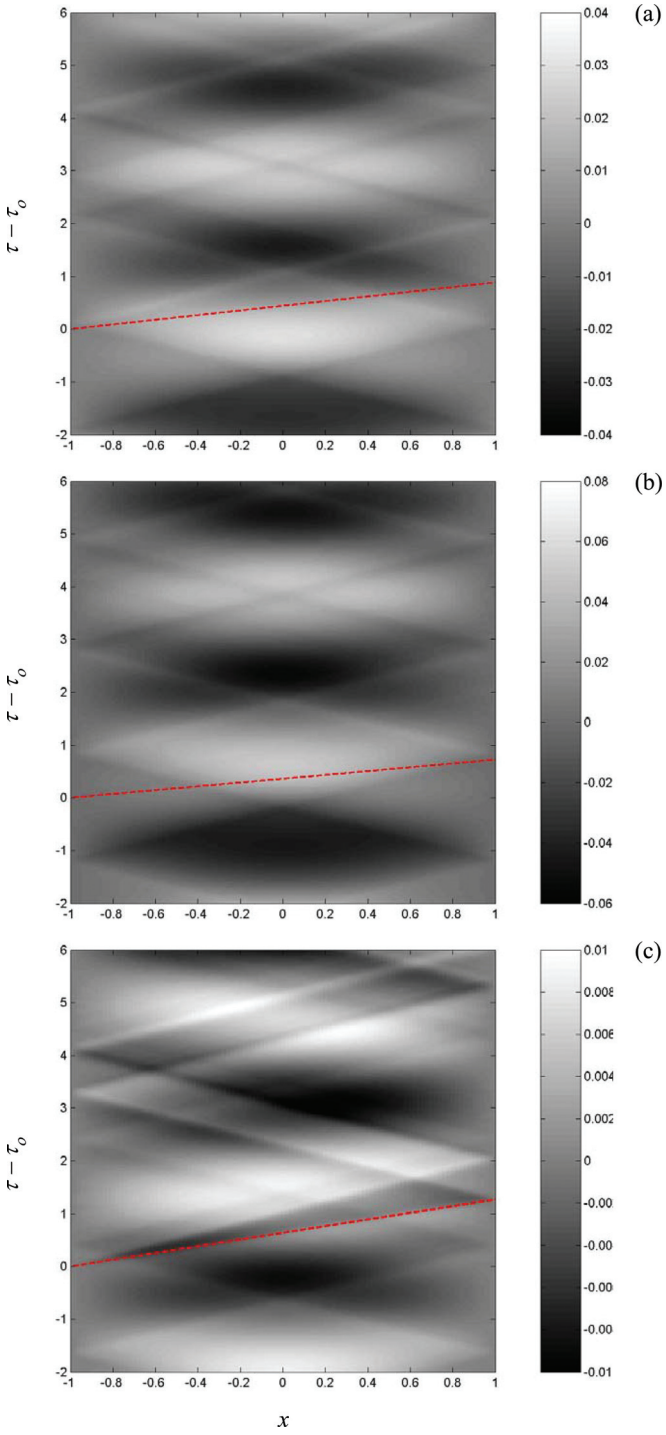

FIG. 3. (Color online) Time variations of lower membrane vibration velocities. (a) $U = 1.5$; (b) $U = 2$; (c) $U = 0.8$. $T = 100$, $m = 100$, and $y_{oi} = 0.1$.

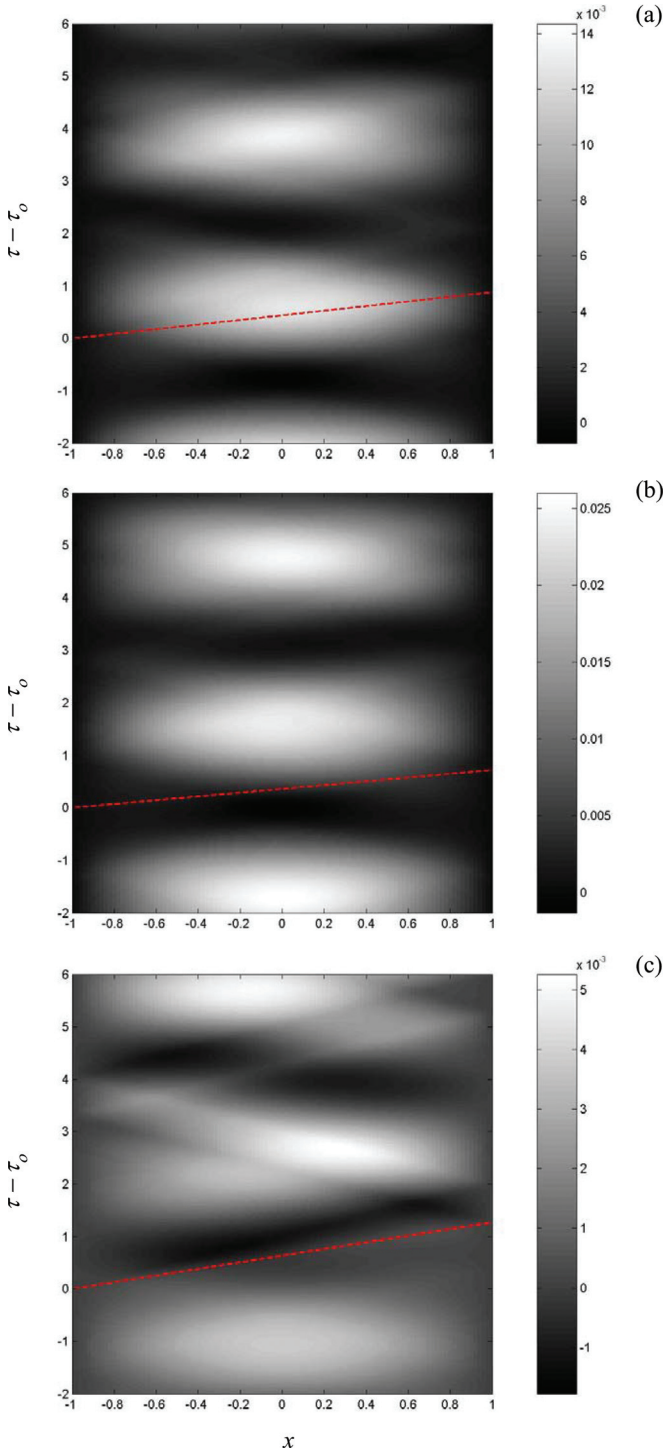

FIG. 4. (Color online) Time variations of lower membrane displacements. (a) $U = 1.5$; (b) $U = 2$; (c) $U = 0.8$. $T = 100$, $m = 100$, and $y_{oi} = 0.1$.

it [Fig. 3(a)]. The strength of the membrane vibration velocity is decreasing during the same period as well. However, the opposite occurs when U is increased to 2 [Fig. 3(b)]. Figure 3(c) shows the vibration velocity of the lower membrane for $U = 0.8$. The vibration velocity of the lower membrane is very weak during its interaction with the vortex.

Figure 4 shows the lower membrane displacements for the three cases discussed in Fig. 3. For $U = 1.5$, the displacement actually reaches its peak when the vortex flies over the middle of the lower membrane [Fig. 4(a)], resulting in a very large increase in the vortex height. This is not the case for $U = 2$ [Fig. 4(b)] or 0.8 [Fig. 4(c)]. The vortex motion therefore depends critically on the phases of the membrane vibrations at the instant the vortex starts interacting strongly with the two membranes. The initial position of the vortex thus affects the vortex path under a non-vanishing U. For $U > 0$, $y_{oi} < 0.5$ and

$$n < f_m|x_{oi} + a|/[U + \cot(\pi y_{oi}/a)\Gamma/(4a)] < (2n + 1)/2, \quad (17)$$

Redistribution subject to ASA license or copyright; see http://acousticalsociety.org/content/terms. Download to IP: 158.132.161.50 On: Fri, 27 Dec 2013 13:08:13

where f_m is the vibration frequency of the membrane and n is an integer, the vortex tends to move upward when it starts interacting vigorously with the membranes. The vortex path tends to bend downward initially otherwise. The vibration frequency f_m is basically not related to U in the range of the latter tested. One can infer from Eqs. (5)–(7) that U and $\partial\gamma/\partial t$, which are coupled with the membrane vibration velocities, are affecting the damping of the system. The fluid loadings, described by the time derivatives of the third and fourth terms on the right-hand-side of Eq. (6), affect the effective mass per unit length of the membrane. Since $\eta_l = -\eta_u$ before the vortex starts integrating with the membranes and the third term, which is expected to be larger, is negative, the fluid loadings tend to reduce the effective mass per unit length of the membrane. Neglecting the non-linear terms and the damping contribution which are expected to be small in the present case, one obtains by considering the membrane motion at $x = 0$ (membrane center) and the observed dominancy of the membrane fundamental mode vibrations before the vortex comes close to the membrane section (Figs. 3 and 4)

$$f_m = \frac{1}{2\pi}\sqrt{\frac{2c^2}{(m+\Delta m)h\pi} + \frac{\pi^2 T}{(m+\Delta m)L^2}}, \tag{18}$$

where Δm denotes the adjustment to the mass per unit length of the membrane due to fluid loading. The present results show that Aw accounts for about 6% of m for $m \leq 100$ and ~12% of m for $m = 200$ (not shown here).

It should be noted that Eq. (18) is not so valid after the vortex starts interacting with the membranes as one can observe that there exist higher vibration modes in the membranes after that instant (Figs. 3 and 4). Figure 5 illustrates the time variations of the amplitudes of the first three vibration modes on the lower membrane for $y_{oi} = 0.1$, $T = 100$, and $m = 50$ with $U = 0.5$ and 1. The corresponding mode shapes are $\cos(\pi x/L)$, $\sin(2\pi x/L)$, and $\cos(3\pi x/L)$, respectively. The

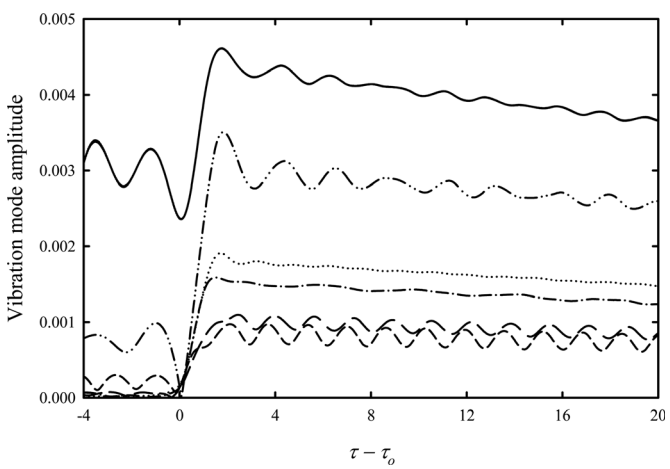

FIG. 5. Examples of lower membrane vibration mode magnitude time variations. ————: First mode $\cos(\pi x/L)$, U=1; — — —: second mode $\sin(2\pi x/L)$, $U = 1$; — —: third mode $\cos(3\pi x/L)$, $U = 1$; — —: first mode $\cos(\pi x/L)$, $U = 0.5$; — —: second mode $\sin(2\pi x/L)$, $U = 0.5$; ·····: third mode $\cos(3\pi x/L)$, $U = 0.5$, $T = 100$, $m = 50$, and $y_{oi} = 0.1$.

vortex induces higher order vibration modes. Though the amplitude of fundamental mode remains the largest among the three modes throughout the interaction, the second mode is more than half than that of the fundamental one after being excited by the vortex motion for $U = 0.5$ and is about ~1/3 for $U = 1$. However, one should note that this second vibration mode, which is an asymmetric one, is not effective in sound radiation.[27] Higher modes become unimportant for $U = 2$ (not shown here). The higher the mean flow velocity, the more dominant the fundamental mode will be. The increase in U also results in slower percentage decay of the mode amplitudes as can be observed from Fig. 5. This counteracting effect between U and D can actually be inferred from Eqs. (6) and (7). In addition, one can notice from Fig. 5 that the stronger the mean flow, the weaker the effect of the vortex on affecting the membrane vibration and thus the sound radiation (discussed later). The increase in m reduces the vibration magnitudes but not the characteristics, and thus the corresponding results are not discussed. Besides, the non-symmetrical velocity induction of the vortex on the two membranes results in a slight shift of the phase relationship between the membrane vibrations (not shown here).

B. Downstream sound radiation

Figure 6 shows two examples of the time variation of the sound pressure far downstream of the membrane section. The sound generated before the vortex comes close to the membrane section observed in Fig. 6(a) is due to the membrane vibration excited by the mean flow alone. The monopole radiations are actually the stronger source for all the cases studied in the present investigation.

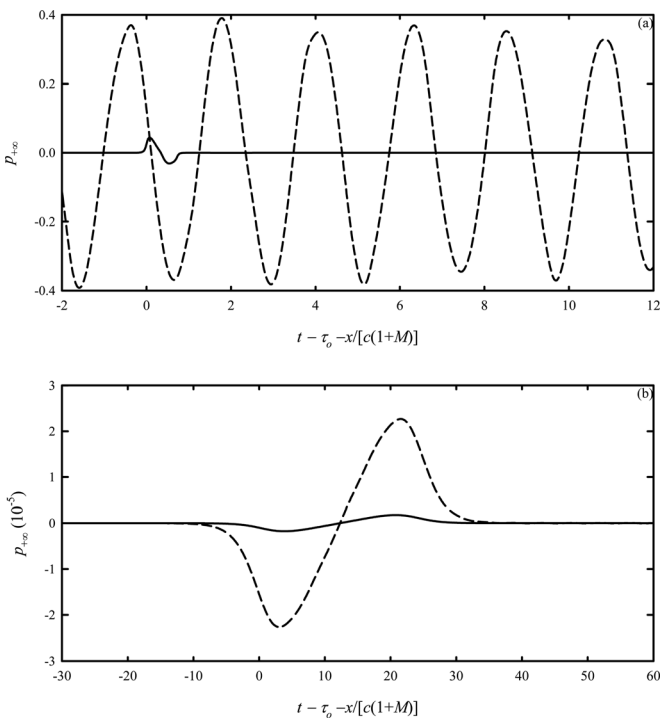

FIG. 6. Contributions of vortex transverse acceleration and membrane vibration to sound generation. $T = 100$. (a) $m = 50$; $y_{oi} = 0.1$ and $U = 2$; (b) $m = 200$; $y_{oi} = 0.4$; and $U = 0$. ————: From vortex transverse acceleration; — — —: overall sound radiation.

Redistribution subject to ASA license or copyright; see http://acousticalsociety.org/content/terms. Download to IP: 158.132.161.50 On: Fri, 27 Dec 2013 13:08:13

The effects of the mean flow magnitude on the time variations of $p_{+\infty}$ for $y_{oi}=0.1$, $T=100$, and $m=50$ are showed in Fig. 7(a). It is noticed that the vortex interaction with the membranes (mostly with the lower one for this y_{oi}) will result in an increase in the sound amplitude for $U<1$ and the effect of the vortex is not significant for larger U. The jump of sound amplitude due to the vortex excitation, if this excitation occurs, decreases with increasing U. Similar phenomenon is also observed for the corresponding cases for $m=200$, but it takes place at a lower U [Fig. 7(b)]. Increasing y_{oi} reduces the influence of the vortex on the membrane vibration and thus gives an effect similar to increasing m on the sound radiation when the vortex effect is still significant compared to that of the mean flow. However, the effect of the vortex excitation cannot be clearly observed when y_{oi} is increased to 0.2 with $T=100$ and $m=50$ [Fig. 7(c)]. For $y_{oi}=0.4$, the pressure fluctuations are just as if there is no vortex even for $c_m=12$ with $U=0.2$ (not shown here). There exists a critical U over which the vortex excitation becomes insignificant compared to the mean flow induction.

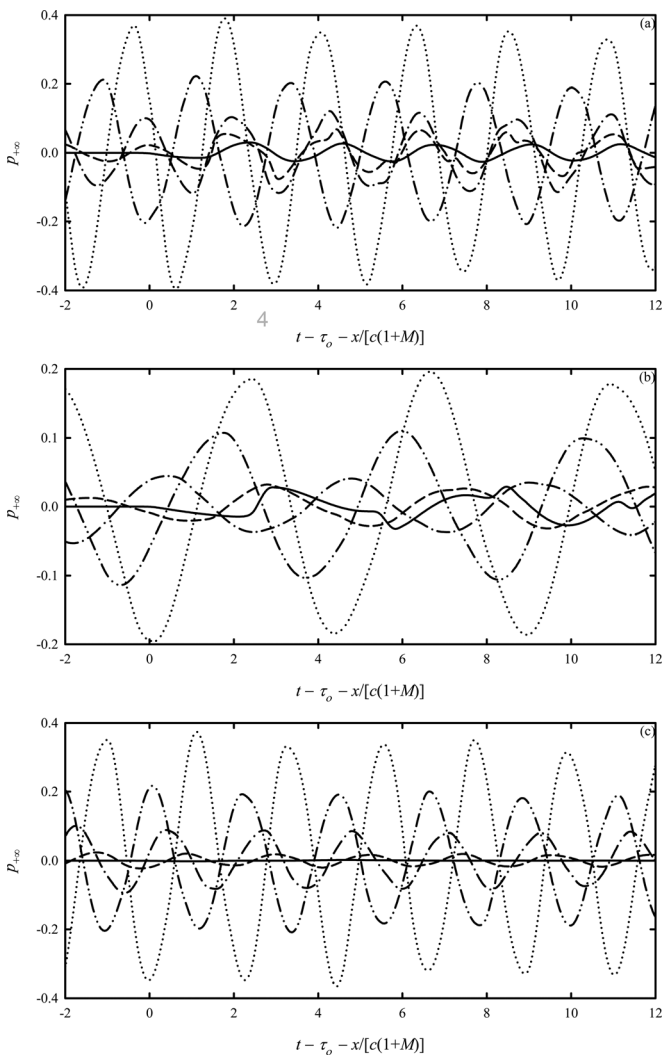

FIG. 7. Effects of mean flow velocity, membrane mass and initial vortex height on sound radiation, $T=100$. (a) $y_{oi}:=0.1$ and $m=50$; (b) $y_{oi}=0.1$ and $m=200$; (c) $y_{oi}=0.2$ and $m=50$. ————: $U=0$; — — —: $U=0.5$; —·—: $U=1$; —··—: $U=1.5$; ·····: $U=2$.

Since the vortex paths and thus the sound radiation depend on the initial location of the vortex, x_{oi} is then varied accordingly so that the effect of membrane vibration phase on the sound radiation can be summarized. Figure 8(a) illustrates the average ratios of the sound amplitudes before and after the vortex interaction and their standard deviations under different combinations of the system parameters because of the effect of x_{oi}. The vortex effect is negligible if this ratio is slightly less than unity and the weak decay is due to damping effect. One can observe that for $y_{oi}=0.1$, where the vortex influence on the membranes is still significant, the vortex passage on average creates an increase in the sound magnitude for $U\leq 1.2$ provided that $c_m=\sqrt{2}$ where the tension effect within the membrane is dominating. Such increase in magnitude decreases as U increases.

A reduction in c_m results in the dominance of the mean flow effect at a lower U. For $y_{oi}=0.1$, this critical U is around 0.8 for $c_m\leq 1$. However, the effect of the vortex is still observable until U becomes larger than 1. The increase in y_{oi} to 0.2 reduces the vortex self-induced speed and its influence on the membranes. However, the critical U is still around 0.8 with reduced standard deviation of the sound amplitude ratio. At a mean flow velocity higher than this critical value, the vortex dynamics are controlled mostly by membrane vibrations created by the mean flow and thus explain the observed large upward motions of the vortex in Fig. 2 which only take place at relatively high U. The further increase of y_{oi} to 0.4 results in the amplitude ratio falling between 0.9 and 1.05. The overall vortex effect is insignificant and thus the corresponding results are not presented.

Figure 8(b) illustrates the average peak sound pressure magnitudes after the vortex passes over the leading edge of the membrane section and their standard deviations for the combinations of parameters adopted in Fig. 8(a). The peak sound pressure magnitude basically increases with U which is expected. As already implied by the results shown in Fig. 8(a), the sound magnitude at high U increases only with increasing c_m and so does the abovementioned critical velocity. One can observe that the standard deviation of the peak sound magnitude does not vary much for $U\geq 0.4$. In addition, the standard deviation of the peak sound magnitude due to the vibration phase effect is only about 4% of the mean peak sound magnitude for $y_{oi}=0.1$ at $U=2$ ($c_m=1$ or $\sqrt{2}$) and is only 2% for $y_{oi}=0.2$, suggesting that the phase effect on the sound radiation will become less important at higher mean flow velocity or when the vortex effect becomes weaker.

C. Effects of asymmetric membranes

The mutual resonating forcing between the membranes is in general absent when the two membranes are not identical. In this section, y_{oi} is fixed at 0.1 as the vortex effect for larger y_{oi} is less prominent as shown in Sec. III B. The initial vortex position x_{oi} is fixed at -10 unless otherwise specified. The suffices u and l again denote quantity associated with the upper and lower membrane, respectively. For the sake of simplicity, $T_l=T_u=100$, while structural damping is ignored ($D_l=D_u=0$).

Redistribution subject to ASA license or copyright; see http://acousticalsociety.org/content/terms. Download to IP: 158.132.161.50 On: Fri, 27 Dec 2013 13:08:13

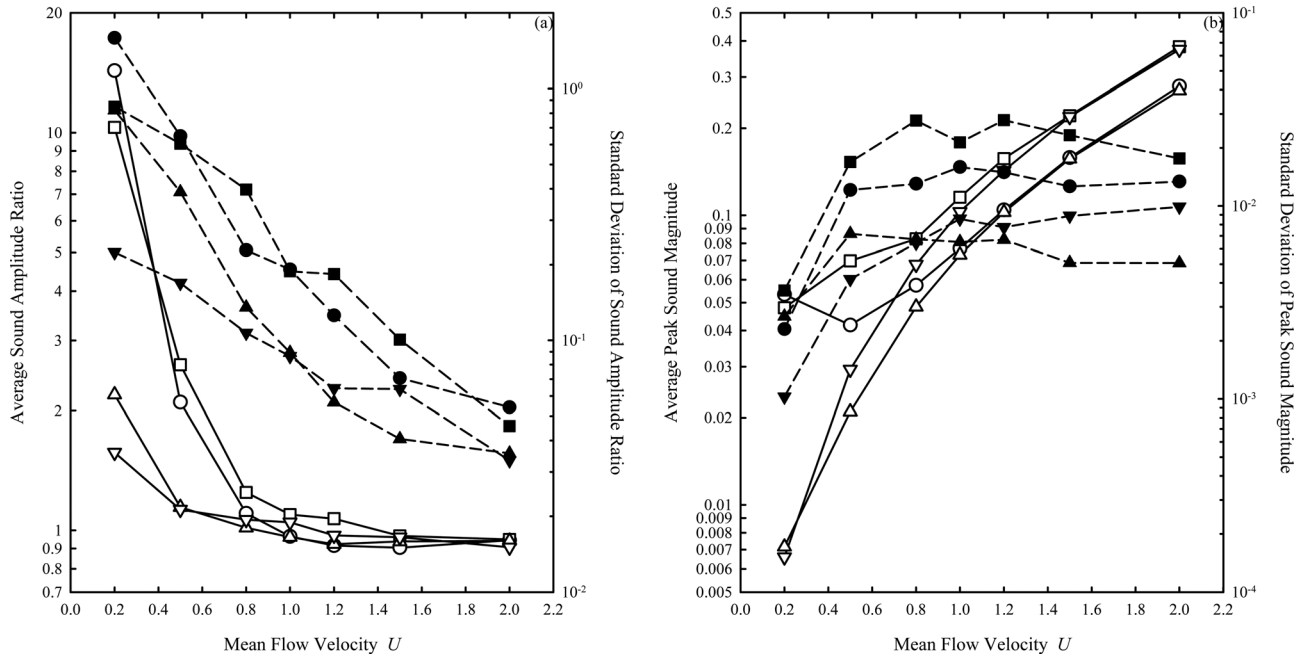

FIG. 8. Combined effects of mean flow velocity, membrane wave speed, and initial vortex height on sound radiation ($T=100$). (a) Sound amplitude ratio; (b) sound amplitude after intensive vortex-membrane interaction. Open symbols: average; closed symbols: standard deviation. •: $m=100$, $y_{oi}=0.1$; ■: $m=50$, $y_{oi}=0.1$; ▲: $m=100$, $y_{oi}=0.2$; ▼: $m=50$, $y_{oi}=0.2$.

Figures 9(a) and 9(b) illustrate the vortex paths with various $c_{m,l}$ but a fixed $c_{m,u}$ of 1 and U of 0.2 for $y_{oi}=0.1$ and 0.2, respectively. At this mean flow velocity, the vortex has a significant effect on the membrane vibrations as concluded from the previous sections. The effect of $c_{m,u}$ at these values of y_{oi} on the vortex path is not significant and thus is not discussed. However, a larger y_{oi} still results in stronger effect of $c_{m,u}$. Figure 9 tends to suggest that larger change in the vortex path can be resulted by reducing the wave speed of the lower membrane for $c_{m,l}\geq 1$. For $y_{oi}=0.2$, extensive vortex path change can even be observed at $c_{m,l}=1/\sqrt{2}$. The change in the wave speed implies a change in the vibration frequency of the lower membrane, and thus the vortex will start interacting with this membrane at different phases of the membrane vibration. However, the very weak mean flow effect compared to that of the vortex makes the phase effect negligible compared to that resulted from the mechanical property change of the lower membrane.

The results for the case with $U=1$ where the mean flow effect on the membrane vibration becomes inferior to that of the vortex are in principle in line with those shown in Fig. 9, but the vortex path bends upward when $U=1$ (not shown here). The much stronger mean flow effect in this case also makes the phase effect more significant than that at $U=0.2$ (discussed later).

In Fig. 10(a), the sound pressure time fluctuations far downstream of the membrane section for $U=0.2$ and $y_{oi}=0.1$ with T_u and m_u both fixed at 100 such that $c_{m,u}=1$ are presented. The variation of $c_{m,u}$ does not produce significant different results, and thus the corresponding data are not presented. Under this condition where the vortex is controlling the membrane vibrations and thus the sound radiation, the frequency of the sound radiated equals that of the lower

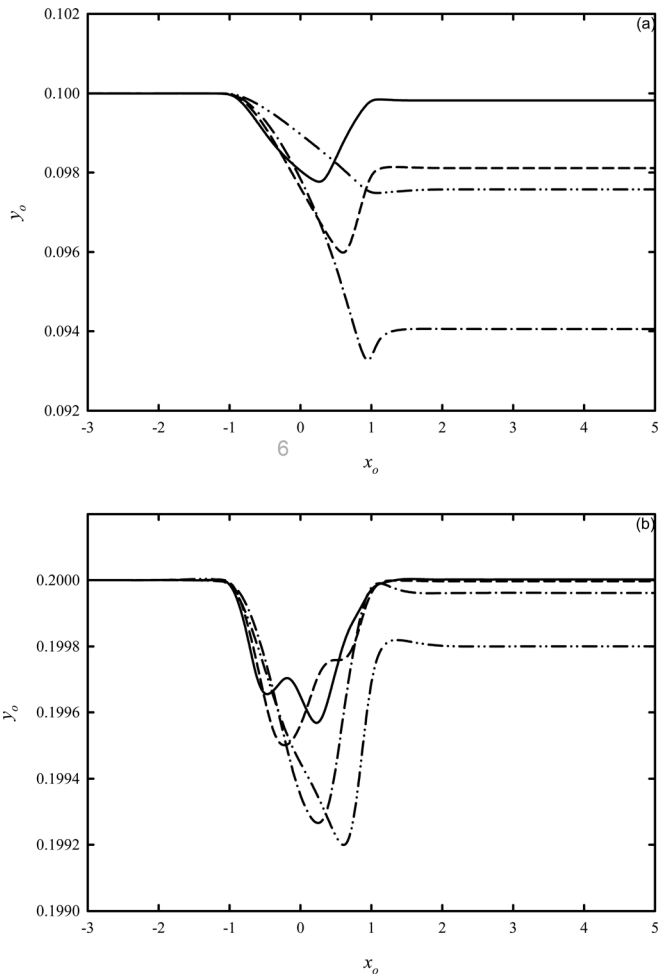

FIG. 9. Examples of vortex paths in the presence of an asymmetric membrane section for $U=0.2$ and $c_{m,u}=1$. (a) $y_{oi}=0.1$; (b) $y_{oi}=0.2$. ————: $c_{m,l}=2$; _ _ _: $c_{m,l}=\sqrt{2}$; —·—: $c_{m,l}=1$; —··—: $c_{m,l}=\sqrt{1/2}$.

Redistribution subject to ASA license or copyright; see http://acousticalsociety.org/content/terms. Download to IP: 158.132.161.50 On: Fri, 27 Dec 2013 13:08:13

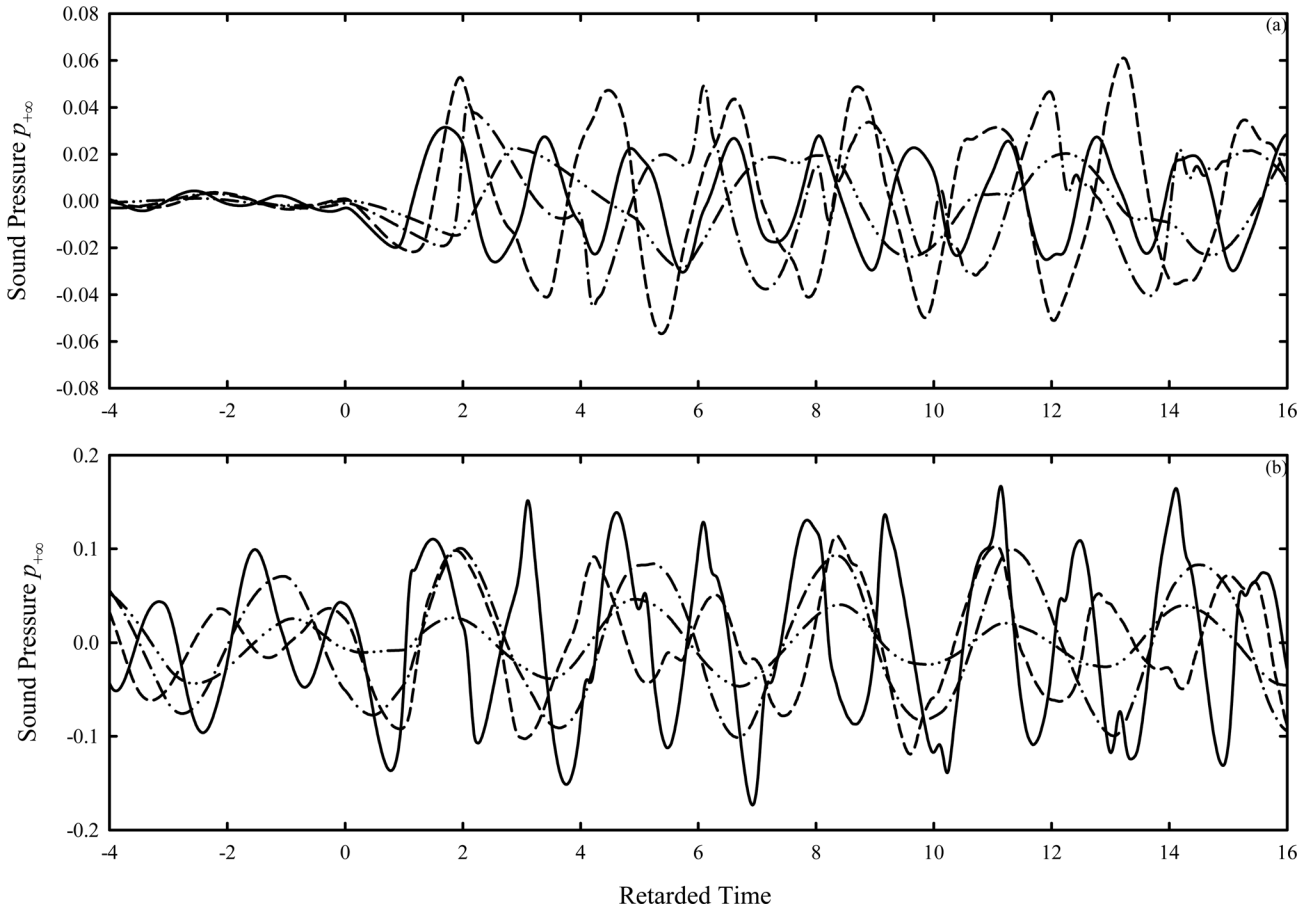

FIG. 10. Time variations of $p_{+\infty}$ radiated from vortex interactions with asymmetric membrane section with $c_{m,u}=1$, $y_{oi}=0.1$, $T_u=T_l=100$. (a) $U=0.2$; (b) $U=1$. Legends: same as those for Fig. 9.

membrane vibration and the radiation is the strongest when $c_{m,l} \sim \sqrt{2}$. This will be discussed further later.

For large U, the membrane vibrations are controlled basically by the mean flow. Some examples of the sound radiation for $U=1$ with other conditions the same as those for Fig. 10(a) are presented in Fig. 10(b). One can observe the stronger sound radiation both before and after the intensive interaction between the vortex and the membranes. However, one can find out from this figure that the frequency of the sound radiation is nearly unchanged for $c_{m,l}<1$, where the sound generated by the lower membrane is weak compared to that of the upper membrane at large U. Unlike the case for small U, the upper membrane does play an important role on the sound radiation process when U becomes large even that the vortex is close to the lower membrane. The initial vortex longitudinal position x_{oi} is also affecting significantly the sound radiation.

Figure 11(a) illustrates the power spectral densities of the strongest sounds radiated at various $c_{m,l}$ with $c_{m,u}$ fixed at 1, $y_o=0.1$ and $U=0.2$ after the vortex has propagated downstream of the membrane section (x_{oi} varies). It can be observed that the radiation is the strongest at $m_l \sim 75$, which corresponds to a $c_{m,l}$ of $\sqrt{4/3}$ and the frequency of the major sound radiated follows that of the lower membrane vibration. Under this low mean flow velocity condition, the upper membrane is not actively contributing to the sound radiation. Resonance does not occur even at a $c_{m,l}$ of unity (such that $c_{m,l}=c_{m,u}$) as the motion of the upper membrane is weak and is mainly driven by the unsteady lower membrane vibration.

Figure 11(b) illustrates the spectra of the strongest sound radiated at different $c_{m,l}$ with $c_{m,u}=1$, $y_o=0.1$, and $U=1$ again after the vortex has left the membrane section. The sound radiated in this case is considerably stronger than those shown in Fig. 11(a) as expected. The stronger mean flow excites the vibrations of the two membranes. For a lighter lower membrane, such vibration is stronger, and thus stronger sound radiated can be expected at lower m_l. However, there is a jump in the radiated sound energy when $c_{m,l}=c_{m,u}$ because of membrane vibration resonance. In fact, one can observe that there are spectral peaks at the upper membrane vibration frequency for all m_l tested, though they are weaker than those at the lower membrane vibration frequency. The latter spectral peaks disappear at x_o of the weakest sound radiation for $c_{m,l}<c_{m,u}$ (not shown here), resulting in the nearly unchanged sound frequency for $c_{m,l}<c_{m,u}$ observed in Fig. 10(b).

The resonant sound radiation is the strongest when $c_{m,u}$ is allowed to vary while $c_{m,l}$ is kept at unity as shown in Fig. 11(c). One can observe from Figs. 11(b) and 11(c) that much stronger sound radiation will be resulted when the vortex moves closer to the membrane with higher c_m.

Figure 12 illustrates the average and the range of the root-mean-square sound pressure p_{rms} after the vortex leaves the membrane section for the various combinations of $c_{m,l}$ and $c_{m,u}$ studied. The presence of a p_{rms} range is due to the

Redistribution subject to ASA license or copyright; see http://acousticalsociety.org/content/terms. Download to IP: 158.132.161.50 On: Fri, 27 Dec 2013 13:08:13

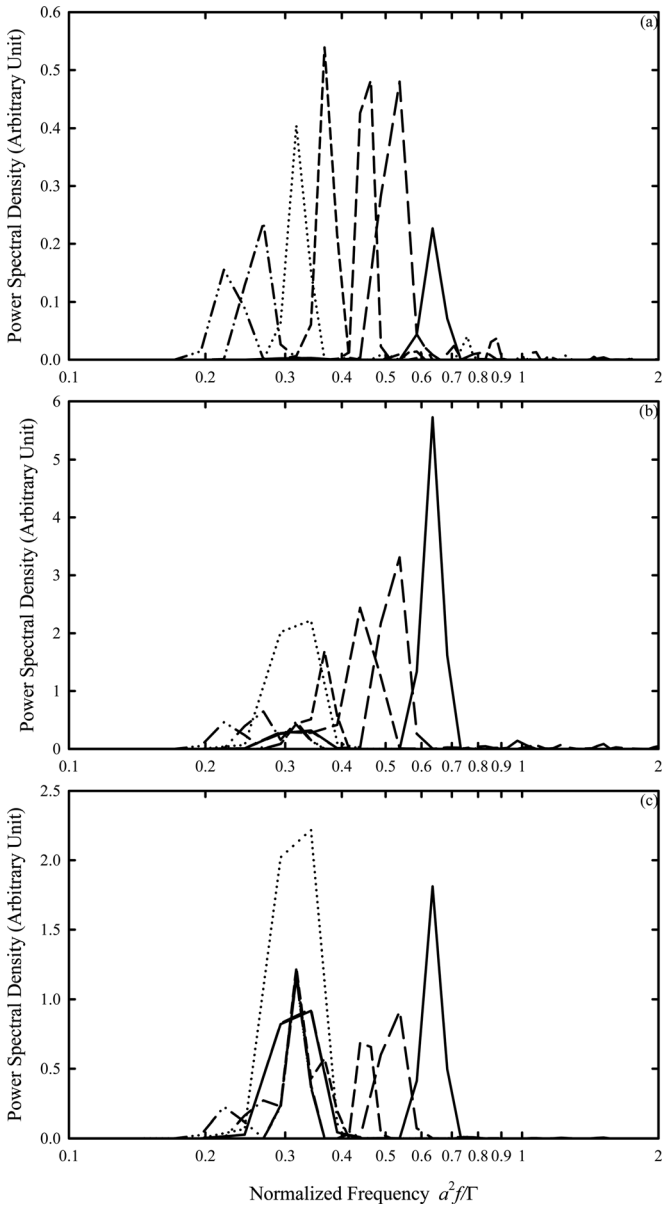

FIG. 11. Spectra of the strongest sounds radiated at different combinations of $c_{m,u}$ and $c_{m,l}$. (a) $U=0.2$, $c_{m,u}=1$; (b) $U=1$, $c_{m,u}=1$; ———: $c_{m,l}=2$; —— ——: $c_{m,l}=\sqrt{8/3}$; — — — : $c_{m,l}=\sqrt{2}$; — — — —: $c_{m,l}=\sqrt{4/3}$; ·····: $c_{m,l}=1$; ——·——: $c_{m,l}=\sqrt{2/3}$; ——.. —— : $c_{m,l}=\sqrt{1/2}$. (c) $U=1$, $c_{m,l}=1$. ———: $c_{m,u}=2$; ___ ___: $c_{m,u}=\sqrt{8/3}$; — — —: $c_{m,u}=\sqrt{2}$; — — — —: $c_{m,u}=\sqrt{4/3}$; ·····: $c_{m,u}=1$; —,—: $c_{m,u}=\sqrt{2/3}$; —..— $c_{m,u}=\sqrt{1/2}$. $y_{oi}=0.1$. $T_u=T_l=100$.

variation of the initial vortex position x_{oi} (thus the vibration phases of the membranes during their close interactions with the vortex), and $p_{\rm rms}$ actually varies very sinusoidally with x_{oi} (not shown here). The $p_{\rm rms}$ range is widened upon an increase in U or in the ratio of $c_{m,l}/c_{m,u}$, but the range is too small to be significant for $U=0.2$.

One can expect for an asymmetric membrane sections that the vibrations of the two membranes may not enhance sound radiation especially when the two wave speeds are very different. Therefore, it is expected that the $p_{\rm rms}$ will not increase monotonically with increasing $c_{m,l}$ when $c_{m,u}$ is fixed even if one excludes the resonance effect. For a weak flow of $U=0.2$, the $p_{\rm rms}$ starts to drop at $c_{m,l}/c_{m,u}\sim 1.15$.

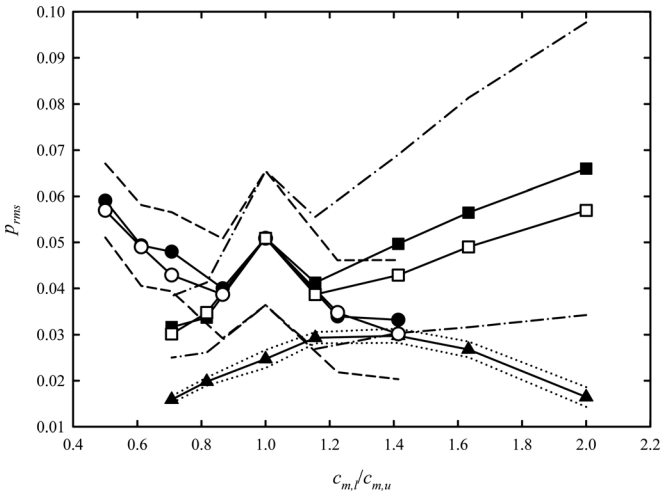

FIG. 12. Effect of membrane *in-vacuo* wave speed ratio on the radiated sound pressure. •: $U=1$, $c_{m,u}=1$; ■: $U=1$, $c_{m,l}=1$; ▲: $U=0.2$, $c_{m,u}=1$; ○: $U=1$, $c_{m,u}=1$ (without vortex); □: $U=1$ $c_{m,l}=1$ (without vortex). — — — —: $p_{\rm rms}$ range for $U=1$, $c_{m,l}=1$; ———·———: $p_{\rm rms}$ range for $U=1$, $c_{m,u}=1$; ·····: $p_{\rm rms}$ range for $U=0.2$, $c_{m,u}=1$; $y_{oi}=0.1$. $T_u=T_l=100$.

The $p_{\rm rms}$ should start to drop at a certain $c_{m,l}/c_{m,u}$ ratio even for $U=1$, but this ratio should have fallen outside the range of the present study. The $c_{m,l}/c_{m,u}$ ratio for the strongest sound radiation is expected to increase with U.

Also shown in Fig. 12 are the $p_{\rm rms}$ due to the mean flow in the absence of the vortex for $U=1$. The resonant sound generation is again observed. In addition, it is noted that the strength of the sound excited by the mean flow alone is almost equal to the mean magnitude of the strongest sound radiation when the vortex is moving closer to the membrane with a fixed wave speed. The presence of the vortex at $U=1$ moderates the vibration magnitude of that membrane, which together with some sound generated by the other membrane, resulting in the variation of $p_{\rm rms}$ at a fixed $c_{m,l}/c_{m,u}$ ratio. The same is also true for the cases where the vortex is moving closer to the heavier membrane. As the variation of $p_{\rm rms}$ with x_{oi} is very sinusoidal (not shown here) when the other parameters are fixed, the chances of strengthening and attenuation of sound radiation due to the presence of a vortex are equal.

For the cases where the vortex is moving closer to the lighter membrane, there will be higher chance for a vortex to enhance the sound radiation. The sound radiated due to a mean flow velocity of 0.2 alone is insignificant (highest $p_{\rm rms}<0.006$), and thus the vortex strengthens very much the sound radiation when the flow speed is low.

IV. CONCLUSIONS

The sound generated by a vortex moving across a section bounded by flexible walls (membranes) inside an otherwise rigid-walled infinitely long two-dimensional duct in the presence of a mean duct flow was investigated in the present study by using the matched asymptotic expansion method after the vortex motions were determined by the potential theory. The effects of the mean flow speed, the membrane mechanical properties, and the vortex initial position on the strength of the radiated sound and its fluctuations were

Redistribution subject to ASA license or copyright; see http://acousticalsociety.org/content/terms. Download to IP: 158.132.161.50 On: Fri, 27 Dec 2013 13:08:13

examined in detail. The major mechanical properties of the membranes considered were the tension per unit spanwise length and the mass density. The initial vortex height was kept below the centerline of the duct and thus the vortex was always closer to the lower membrane. The present setup is in analogy with the configuration of a membrane-based duct silencer in the presence of a low Mach number flow.

The results illustrate that the major sound generation mechanisms are the transverse acceleration of the vortex and the rate of change of the volumetric flow developed by the vibrating membranes. The latter is the dominant source and is affected by both the vortex motion and the mean flow. In general, an increase in the mean flow will give an increase in sound radiation.

For the cases of symmetric membranes, there exists a critical mean flow velocity above which the effect of the mean flow in affecting the membrane vibrations and the sound radiation becomes dominating. This critical velocity is only weakly dependent on the mechanical properties of the membranes but will definitely be reduced as the vortex is further away from the lower membrane (weaker vortex induced membrane vibration). At low mean flow condition, the vortex excites the membrane vibrations, which eventually generates the sound. At velocities above the critical value, the membrane vibrations driven by the mean flow result in strong sound radiation and the instant at which the vortex starts the vigorous interaction with the membranes (thus the phase of membrane vibration at that instant) is crucial as such additional excitation can enforce or attenuate the mean flow excited membrane vibrations.

The observations for the symmetric membranes basically apply to the cases of asymmetric membranes, where the resonating mutual forcing between the membranes at stronger mean flows does not exist. The results tend to suggest that the sound radiation will be the strongest at a particular ratio of the membrane *in-vacuo* wave speeds except at the point of resonance (identical membranes) and this critical ratio is expected to increase with the mean flow velocity. Resonance is not observed at low mean flow velocity where the vortex effect on the membrane vibration dominates.

It is also observed that the introduction of a vortex will always strengthen the sound radiation when the mean flow is low regardless the initial vortex longitudinal position. In the case of a continuous vortex stream forcing the membrane vibrations, the present results tend to suggest that there is a higher chance of the sound radiation being amplified when the vortex stream is closer to the lighter membrane and the mean flow is relatively strong or when the mean flow is weak. For the other cases, the chances of sound amplification and attenuation by the vortices are equal, and thus the overall effect is not expected to be significant.

Since the introduction of the mean flow will result in sound radiation, the performance of a drum-like silencer is likely to degrade in the presence of the duct flow. For a duct flow speed much less than the membrane wave speeds, a symmetric membrane setup and a low turbulence level are recommended. However, an asymmetric membrane setup should be used when the flow speed is comparable to the membrane wave speeds to avoid resonance. Also, as the turbulence level is more-or-less uniform in a practical flow duct, a 20% difference between the wave speeds of the two membranes is believed to be the optimal option.

ACKNOWLEDGMENT

The financial support from the Research Committee, The Hong Kong Polytechnic University is gratefully acknowledged (G-U906).

[1]C. M. Harris, *Handbook of Noise Control* (McGraw-Hill, New York, 1979), Chap. 29.
[2]U. Ingard, "On the theory and design of acoustic resonators," J. Acoust. Soc. Am. **25**, 1037–1061 (1953).
[3]M. L. Munjal, *Acoustics of Ducts and Mufflers* (Wiley, New York, 1987), pp. 1–305.
[4]A. Selamat, I. J. Lee, and N. T. Huff, "Acoustic attenuation of hybrid silencers," J. Sound Vib. **262**, 509–527 (2003).
[5]G. Canevet, "Active sound absorption in an air conditioning duct," J. Sound Vib. **58**, 333–345 (1978).
[6]P. A. Nelson and S. J. Elliott, *Active Control of Sound* (Academic Press, London, 1992), pp. 120, 161–203.
[7]R. D. Ford and M. A. McCormick, "Panel sound absorbers," J. Sound Vib. **10**, 411–423 (1969).
[8]A. Frendi, L. Maestrello, and A. Bayliss, "Coupling between plate vibration and acoustic radiation," J. Sound Vib. **177**, 207–226 (1994).
[9]P. J. T. Filippi, O. Lagarrigue, and P.-O. Mattei, "Perturbation method for sound radiation by a vibrating plate in a light fluid: Comparison with the exact solution," J. Sound Vib. **177**, 259–275 (1994).
[10]L. Huang, "A theoretical study of duct noise control by flexible panels," J. Acoust. Soc. Am. **106**, 1801–1809 (1999).
[11]L. Huang and Y. S. Choy, "Vibro-acoustics of three dimensional drum silencer," J. Acoust. Soc. Am. **118**, 2313–2320 (2005).
[12]A. P. Dowling, "Sound generation by turbulence near an elastic wall," J. Sound Vib. **90**, 309–324 (1983).
[13]S. K. Tang, R. C. K. Leung, R. M. C. So, and K. M. Lam, "Acoustic radiation by vortex induced flexible wall vibration," J. Acoust. Soc. Am. **118**, 2182–2189 (2005).
[14]J. E. Ffowcs Williams, "The acoustics of turbulence near sound-absorbent liners," J. Fluid Mech. **51**, 737–749 (1972).
[15]S. K. Tang and C. K. Lau, "Two-dimensional model of low Mach number vortex sound generation in a lined duct," J. Acoust. Soc. Am. **126**, 1005–1014 (2009).
[16]D. G. Crighton, "Radiation from vortex filament motion near a half-plane," J. Fluid Mech. **51**, 357–362 (1972).
[17]M. S. Howe, *Acoustics of Fluid-Structure Interactions* (Cambridge University Press, Cambridge, 1998), pp. 157–410.
[18]F. Obermeier, "The influence of solid bodies on low Mach number vortex sound," J. Sound Vib. **72**, 39–49 (1980).
[19]S. K. Tang, R. C. K. Leung, and R. M. C. So, "Vortex sound due to a flexible boundary backed by a cavity in a low Mach number mean flow," J. Acoust. Soc. Am. **121**, 1345–1352 (2007).
[20]H. R. Vallentine, *Applied Hydrodynamics* (Butterworth, London, 1969), pp. 202–203.
[21]P. Cannell and J.E. Ffowcs Williams, "Radiation from line vortex filaments exhausting from a two-dimensional semi-infinite duct," J. Fluid Mech. **58**, 65–80 (1973).
[22]N. Peake, "On the unsteady motion of a long fluid-loaded elastic plate with mean flow," J. Fluid Mech. **507**, 335–366 (2004).
[23]Y. S. Choy and L. Huang, "Effect of flow on the drumlike silencer," J. Acoust. Soc. Am. **118**, 3077–3085 (2005).
[24]M. S. Howe, "On the stability of boundary-layer flow over a spring-mounted piston," J. Fluid Mech. **125**, 59–73(1982).
[25]W. Möhring, and W. Eversman, "Conversion of acoustic energy by lossless liners," J. Sound Vib. **82**, 371–381 (1982).
[26]J. E. Ffowcs Williams and M. S. Howe, "The generation of sound by density inhomogeneities in low Mach number nozzle flows," J. Fluid Mech. **70**, 605–622 (1975).
[27]M. C. Junger and D. Feit, *Sound, Structures, and Their Interaction* (Acoustical Society of America, Atlanta, 1993), pp. 119–126.

Redistribution subject to ASA license or copyright; see http://acousticalsociety.org/content/terms. Download to IP: 158.132.161.50 On: Fri, 27 Dec 2013 13:08:13